Published in final edited form as:
Curr Pharm Biotechnol. 2014 October ; 14(8): 743–752.

Ultrasound and Microbubble Guided Drug Delivery: Mechanistic Understanding and Clinical Implications

Tzu-Yin Wang, **Katheryne E. Wilson**, **Steven Machtaler**, and **Jürgen K. Willmann***
Department of Radiology, Molecular Imaging Program at Stanford, Stanford University, School of Medicine, Stanford, California, USA

Abstract

Ultrasound mediated drug delivery using microbubbles is a safe and noninvasive approach for spatially localized drug administration. This approach can create temporary and reversible openings on cellular membranes and vessel walls (a process called “sonoporation”), allowing for enhanced transport of therapeutic agents across these natural barriers. It is generally believed that the sonoporation process is highly associated with the energetic cavitation activities (volumetric expansion, contraction, fragmentation, and collapse) of the microbubble. However, a thorough understanding of the process was unavailable until recently. Important progress on the mechanistic understanding of sonoporation and the corresponding physiological responses *in vitro* and *in vivo* has been made. Specifically, recent research shed light on the cavitation process of microbubbles and fluid motion during insonation of ultrasound, on the spatio-temporal interactions between microbubbles and cells or vessel walls, as well as on the temporal course of the subsequent biological effects. These findings have significant clinical implications on the development of optimal treatment strategies for effective drug delivery. In this article, current progress in the mechanistic understanding of ultrasound and microbubble mediated drug delivery and its implications for clinical translation is discussed.

Keywords

Contrast agents; drug delivery; microbubbles; sonoporation; therapy; ultrasound

INTRODUCTION

Ultrasound has been widely applied in the clinics for biomedical imaging because it is a safe, cost-effective, non-invasive, and non-ionizing modality. Medical ultrasound imaging most often uses a frequency range of 1 to 20MHz. This range allows ultrasound to penetrate several (up to 15) centimeters deep into the body without significant signal attenuation and

*Address correspondence to this author at the Department of Radiology and Molecular Imaging Program at Stanford, School of Medicine, Stanford University, 300 Pasteur Drive, Room H1307, Stanford, CA 94305-5621; Tel: 650-723-5424; Fax: 650-723-1909; willmann@stanford.edu.

Send Orders for Reprints to reprints@benthamscience.net

CONFLICT OF INTEREST
The authors confirm that this article content has no conflicts of interest.

distortion. Body images can be formed with good image quality and spatial resolution for diagnostic purposes. The spatial resolution of the image is approximately 0.1 to 1.5 mm, depending on the ultrasound pulse parameters and transducer geometry [1].

While low energy (0.1 – 100 mW/cm^2) ultrasound is used for diagnostic imaging, higher energy ultrasound (100 – 10,000 W/cm^2) is investigated for non-invasive therapies [2]. In ultrasound therapy, the acoustic energy is deposited in a small (1 to 10 millimeters) focal region, causing various therapeutic effects, such as thermal tissue coagulation [3], kidney stone comminution (lithotripsy) [4], mechanical tissue disruption (histotripsy) [5], bone healing [6], modulation of neural activities [7], and many other therapeutic effects [8–10]. The focusing capability allows for treatment in a localized region, minimizing damage to the surrounding healthy tissues. The non-invasive procedure significantly reduces possible complications that may occur in other more invasive surgical procedures. These advantages make therapeutic ultrasound a favorable alternative when applicable.

Among the various therapeutic applications, ultrasound mediated drug delivery has drawn much research attention in the past few decades. Ultrasound mediated drug delivery can be achieved via thermal (hyperthermia) or mechanical mechanisms. Hyperthermia has been shown to cause increased tumor blood flow [11, 12] and increased vascular permeability [13–15], which may assist therapeutic delivery into tumors [16]. Cho *et al.* demonstrated *in vitro* that ultrasound induced hyperthermia enhanced the permeability of hydrophobic molecules into bovine brain microvessel endothelial cells on culture plates [17]. *In vivo*, Watson *et al.* further demonstrated in tumors established on mice that ultrasound induced hyperthermia enhance nanoparticle accumulation by decreasing the intratumoral pressure and increasing the vascular permeability [18]. Additionally, ultrasound hyperthermia can be combined with temperature sensitive liposomes to further enhance therapeutic effects [11,19,20]. Temperature sensitive liposomes can stably carry drugs in the bloodstream and are triggered to release the drugs in the targeted region when the local temperature is increased by ultrasound hyperthermia. This combination can significantly enhance drug delivery compared to using ultrasound or liposome alone, and has been tested *in vivo* to show enhanced localized drug delivery in rabbit muscles [21], tumors on rabbits [22], and tumors on rats [23]. Although enhanced drug delivery using hyperthermia was observed in the above studies, contradictory results were reported in other studies [24, 25].

A more widely investigated approach of ultrasound mediated drug delivery is achieved using mechanical mechanisms. This approach uses ultrasound and gas-encapsulated microbubbles to induce openings on a nearby surface, allowing for increased permeability across natural barriers such as the cell membrane, vessel wall, and the blood brain barrier (Fig. 1). This phenomenon is termed sonoporation. The permeability change caused by sonoporation can be temporary and reversible, allowing for restoration of physiological defense mechanisms after successful drug delivery.

Feasibility of therapeutic use of this technique *in vivo* has been investigated in preclinical animal studies, many of which have demonstrated effective treatment outcomes. For examples, Fujii *et al.* used this technique to suppress tumor angiogenesis for cancer therapy [26]. The vascular endothelial growth factor receptor-2 (VEGFR2) short hairpin (sh)RNA

was delivered to knock down vascular endothelial growth factor (VEGF) for anti-angiogenic treatment. Following ultrasound guided targeted knockdown of VEGF, reduced tumor blood flow could be observed. Tsai *et al.* used this technique to deliver an angiogenic inhibitor, endostatin, into hepatocellular tumors established on mice, and observed substantial tumor growth suppression [27]. Chen *et al.* investigated the potential of using this technique for treatment of diabetes in a rat model [28]. The authors manufactured lipid-shelled microbubbles loaded with therapeutic plasmids, rat insulin 1 promoter (RIP)-human insulin or RIP-hexokinase I plasmids. While RIP was used to achieve specific targeting to the islet beta cells, successful delivery of the human insulin and hexokinase I could help regulate blood glucose levels. Following treatment with the infusions of plasmid loaded microbubbles and exposure to 1.5-MPa 1.3-MHz ultrasound pulses for 20 minutes, a significant increase in serum insulin and decrease in serum glucose was observed at days 5 and 10 in that study [28]. Another important application of this technique is drug delivery across the blood brain barrier for treatment of central nervous system diseases, since alternative treatments are rather invasive or ineffective [29]. Treat *et al.* demonstrated that sonication with microbubbles may enhance delivery of antitumor drugs, doxorubicin, into brain tumors established on mice, resulting in reduced tumor growth and prolonged survival time [30]. Ting *et al.* further demonstrated that the use of drug bearing microbubbles can achieve the same antitumor effects shown by Treat *et al*, i.e., reduced tumor growth, while minimizing systemic drug toxicity [31]. More comprehensive summaries of preclinical studies on ultrasound mediated drug or gene delivery can be found elsewhere [32–36].

This review article focuses on ultrasound and microbubble mediated drug delivery using mechanical effects of ultrasound. Despite encouraging results in preclinical *in vivo* experiments, the underlying mechanisms of ultrasound and microbubble mediated drug delivery remained unclear until recently, and, so far, this technique has not yet been clinically translated. Recent research made significant progress towards understanding the underlying phenomena of ultrasound mediated drug delivery, particularly in terms of the temporally resolved dynamic interactions between micro-bubbles and cells/tissues, critical distance for microbubble-cell or microbubble-tissue interactions, and the temporal therapeutic window for drug delivery following ultrasound insonation. We summarize the recent findings and discuss their potential implications for future clinical applications. The improved understanding on interactions between the microbubble activities and the cells/tissues may help translate this technique into the clinic.

Microbubbles: Key Agents in Sonoporation

Microbubbles play an important multi-functional role in ultrasound mediated drug delivery. These microbubbles are currently used as contrast agents for preclinical and clinical ultrasound imaging to enhance the contrast between blood (in which the microbubbles circulate) and the surrounding tissues [37–41]. They are typically 1 – 4 μm in diameter and comprised of a biologically inert gas (e.g., perfluorocarbon) stabilized in a lipid, protein, or polymer shell. When microbubbles are exposed to the alternating compressional and rarefractional phases of ultrasound, they undergo volumetric contraction, expansion, fragmentation, coalesce, dissolution, and/or violent collapse (Fig. 2a), a process called cavitation [42]. These motions of microbubbles may induce local fluid flow called

"microstreaming" (Fig. 2c) [43–44]. When violent collapse of microbubbles occurs, fast-moving fluid jets may form, which impinge into a nearby surface (Fig. 2b) [45]. These microbubble motions occur very rapidly on the scale of microseconds, and have been investigated theoretically and experimentally by many research groups [46–52]. More details on the microbubble physics during insonation can be found elsewhere [53–55].

Ultrasonically induced microbubble cavitation and fluid motion are believed to cause disruptions of nearby physical structures and enhance subsequent transport of molecules across physiological barriers such as cell membranes, as observed by many researchers. For example, Skyba *et al*. treated an exteriorized rat spinotrapezius muscle with ultrasound and microbubbles in *in vivo* conditions and observed ruptured capillaries with extravasation of red blood cells and nonviable cells in the adjacent tissues post treatment [56]. Despite convincing evidence of tissue disruption post ultrasound and microbubble treatment, the underlying mechanisms of tissue damage were not addressed in that study.

To further assess the underlying mechanisms that cause tissue damage following ultrasound and microbubble treatment, Prentice *et al.* studied microbubble dynamics near a cell surface using high speed photography [57]. The authors observed fluid jets impinging into cells with a 16-μm rupture hole measurable on the cell membrane using atomic force microscopy. From that study it was hypothesized that membrane ruptures following ultrasound and microbubble treatment were caused by fluid jets. Similarly, Ohl *et al*. studied microbubble cavitation on cells adhered to a substrate [58]. They found three distinct effects in three regions: at the center of the collapse, cells were detached by the strong shear stress caused by microstreaming; at the edge of the detachment sites, cells were severely damaged with permanent pores on the membrane; at some distance from the detachment sites, cells remained viable with a clear uptake of a membrane impermeable fluorophore, calcein, from the medium. This study illustrates a key role of cavitation in sonoporation and also suggests involvement of microstreaming in the process.

Microstreaming has been shown to cause membrane disruption by several researchers. Nyborg and Miller theoretically calculated the shear stress caused by microstreaming near a cavitating microbubble, and experimentally observed lysis of red blood cells near the cavitating microbubble [59]. Marmottant and Hilgenfeldt traced the fluid motion and recorded the disruption of a lipid vesicle near a cavitating microbubble [60]. Interestingly, microstreaming can also help the transport of external substances across biological barriers as it can create local flow patterns that attract particles into the proximity of the insonated cells. Such trapping effects may propel the transport of substances across biological barriers by orders of magnitude over diffusive transport [61], which can be leveraged for ultrasound guided drug delivery.

It is worth mentioning that in addition to being the causative agents for barrier disruption, the microbubbles can also serve as drug delivery vehicles which stably carry drugs in the blood circulation. Drugs can be loaded on the microbubble shell, embedded in the shell matrix, or loaded in the internal void (Fig. 3a). The surface of microbubbles can further be functionalized with ligands that specifically bind to receptors at the target region, thereby increasing focal microbubble attachment and local drug concentration. Upon disruption of

microbubbles by ultrasound, a high dose of drugs are released only in the sonicated region (Fig. 3b). This system allows for non-invasive targeted release of drugs while minimizing systemic toxicity to the rest of the body, making it a highly beneficial drug delivery system. The chemistry of the targeted drug-loaded microbubbles is beyond the scope of this article and can be found elsewhere [62–65].

Temporally Resolved Dynamic Interactions between Cavitating Microbubbles and Cells/Tissues

Despite the general perception on causative relation between microbubble cavitation and ultrasound mediated drug delivery, a clear understanding on the temporal dynamic interaction between microbubbles and cells/tissues was not available until recently. Recent studies have made important progress in this regard.

At a single cell level, Fan *et al.* [66] and Kudo *et al.* [67] performed elegant *in vitro* studies on the time-resolved cell-microbubble interaction during cavitation. In both studies, high speed photography and fluorescence microscopy were used to observe the microbubble dynamics and cellular response following ultrasound insonation. Propidium iodide (PI), an agent which only produces fluorescence when entering cells through disrupted membranes, was used as an indicator of sonoporation. By monitoring the spatio-temporal change of the intracellular fluorescence, both groups observed that cell membranes were disrupted at the sites of microbubble induced cavitation and rapidly resealed within several seconds. Fan *et al.* estimated the size of the membrane rupture by fitting the intracellular PI diffusion profile to a quasi-steady electro-diffusion model [68], and suggested the sonoporation induced ruptures may be as small as several nanometers in diameter. Kudo *et al* examined the cellular membrane with electron microscopy and found that larger ruptures up to 1 micron can be generated by sonoporation. Interestingly, the process of pore formation and resealing may be highly controllable by carefully manipulating the cavitation conditions. For example, by increasing cavitation events (induced by higher pressure, the use of larger numbers of microbubbles, or repetitive ultrasound exposure), multiple and/or prolonged membrane disruptions can be induced. Under well-controlled treatment conditions (pressure and durations), the cells remained viable post ultrasound exposure. These studies suggest that cell disruption can be spatially and temporary well-controlled and be reversible, allowing for successful drug delivery without permanent cellular damage.

While the aforementioned studies provide insight into the dynamic interaction between cavitating microbubbles and cells for successful cellular drug delivery in a well-controlled *in vitro* setup, successful drug delivery in an *in vivo* environment is more complex and challenging. For a drug to reach the target cells *in vivo*, several biological barriers have to be overcome. For example, in cancer therapy, certain cancer cell targeted drugs need to first penetrate through the vessel wall, then diffuse into the interstitial space, and finally pass the cancer cell membranes. Furthermore, the cavitation dynamics of microbubbles may be altered *in vivo* compared to *in vitro* settings due to the confinement from the surrounding tissues.

To investigate the cavitation of microbubbles in a tissue environment, Caskey *et al.* studied the expansion, oscillation, and collapse of microbubbles in small (< 30μm) blood vessels in

an *ex vivo* rat mesentery model using a high speed camera with a frame rate of 1000 frames per second. They observed constrained expansion and oscillation of microbubbles in the mesenteric vessels compared to those in the 200μm artificial vessels (cellulose tubes). In the mesenteric vessels, the fusion of small microbubbles into larger (>4μm) microbubbles was critical for the microbubbles to interact with the vessels. Vessel distention of 2.3 μm and invagination of 1.1 μm was observed during the expansion and contraction of the microbubbles. Although the microbubble-vessel interactions were illustrated, histological examinations on the affected vessels were not provided in that study.

Chen *et al.* [69, 70] studied microbubble cavitation in *ex vivo* vessels using a similar tissue model, but at a much higher ultrasound pressure (0.8 – 7.2MPa) compared to the previous study (<2MPa). Using the higher pressures, more significant vessel distention (up to 10 μm) and invagination (up to 25 μm) were observed. The vessels returned to their original size on the order of milliseconds after insonation. Moreover, they found that vessel distention or invagination was highly dependent on the distance between microbubbles and the vessel walls. In relatively larger vessels, i.e., vessel diameter (D) exceeding 2 times maximum microbubble radius (R_{max}), the dominant response was vessel invagination; in smaller vessels ($D < 2R_{max}$,), the dominant response was vessel distention. To examine the bioeffects of these microbubble-vessel interactions, the vessels were preserved for histological analysis or transmission electron microscopy post treatment. Significant damage to the endothelial cells in a region of approximately 60 μm was observed long after a single microbubble cavitation event. Such damage was highly associated with vessel invagination, and occurred when the invagination was more than 50% of the initial radius [71].

Overall, these studies in tissue environment demonstrate the feasibility of inducing effective and controllable cavitation and vessel disruption in biological tissues. More importantly, they indicate a critical point for effective interactions between the microbubbles and the tissues: the distance between the microbubbles and the targeted cells/tissues.

Critical Distance for Microbubble-cell or Microbubble-tissue Interactions

In the aforementioned studies performed by Fan *et al.* [66] and Kudo *et al.* [67], microbubbles were brought in close proximity to the target cells, either by surface modification of microbubbles which allowed the microbubbles to bind to the cell membrane, or by floating the microbubbles to the cells cultured in the ceiling of the experimental chamber. This raises the question whether there is a critical distance needed between the microbubble and cell to induce sonoporation.

Le Gac *et al.* studied the critical distance for sonoporation on a single cell [72]. The authors observed a high (>75%) probability of sonoporation when the cell was within 75% of the maximum microbubble radius. This indicates that for typical microbubbles with 1 to 4 μm in diameter undergoing volumetric expansion to 20 μm, the critical distance to affect the vessel wall is 15 μm. Since the microvasculature in the tumor can be less than 20 μm in diameter [73], it is likely that the microbubble cavitation in these small vessels could affect the vessel wall regardless of whether the microbubbles are targeted/attached to the tumor vasculature or not.

In light of the concept of the critical distance for sonoporation, several approaches to enhance drug delivery were proposed where microbubbles are brought in close proximity to the target cells/tissues for effective interactions. This can be achieved by physically pushing them toward the cell/tissue surface using acoustic radiation force and/or chemically binding them to the cell surface at the target sites. Shortencarier *et al.* [74] described a special pulse sequence comprised of a low-pressure (50 kPa) long-duration (3.3 seconds) radiation force generation pulse followed by three high-intensity (2 MPa) short-duration (3.3 μs) microbubble fragmentation pulses. While the radiation force generation pulse pushed the microbubbles into the proximity of the cells, the fragmentation pulses triggered release of content (fluorescent dye) from microbubbles into the cells. They observed that this combination can induce substantially higher dye delivery than radiation force pulses alone or fragmentation pulses alone in an *in vitro* cell culture setting and in excised rat cecum *ex vivo*.

An alternative approach to bring the microbubbles to the close proximity of the target tissues is to coat the microbubbles with specific ligands which can adhere to the surface of the targeted cells. *Xie et al*. [75] tested this approach by comparing the *in vivo* gene delivery outcomes using microbubbles with and without the capability of targeting to P-selectin on the vessel walls in an ischemic hindlimb model in mice. Interestingly, although the binding capability had no significant effects when applying high pressure (≥1 MPa) ultrasound, it enhanced gene delivery by 5 fold when using low pressure ultrasound (0.6 MPa). One possible explanation for the observation made by Xie *et al.* could be that at high pressures, the microbubbles expand to a larger volume and become closer to the vessel walls. Therefore, vessels can be affected with or without the targeting capability of the microbubbles. At low pressure, the spatial extent of sonoporation is reduced. In this case, juxtaposition of microbubbles and target tissues becomes helpful in the low pressure regime.

Temporal Therapeutic Window for Drug Delivery

While the spatial distance between microbubbles and targeted cells/tissues has been shown to be an important factor for effective drug delivery, the temporal therapeutic window for drug delivery post ultrasound exposure is another equally important aspect which has been investigated in recent studies.

One unique feature of sonoporation is that the permeability change can be temporary and reversible under well-controlled cavitation conditions. This unique feature is beneficial because it allows for restoration of physiological defense mechanisms after successful drug delivery. Determining and creating an appropriate and optimal time window for sufficient drug delivery is critical for designing treatment strategies using ultrasound and microbubbles.

The permeability change can last for from a few seconds to a few hours, depending on the experimental conditions (ultrasound parameters, amount of microbubbles, types of cells/tissues, etc.). At a single cell level, Fan *et al.* [66] showed that a short (8-μs) low intensity (0.17MPa) ultrasound pulse can cause enhanced cellular uptake of PI dye for several minutes (Fig. 4a). In an *in vitro* cell culture experiment, Van Wamel *et al.* [76] measured the cellular uptake of 10 – 70 kDa fluorescent labeled-dextran at different time points after

treatments with microbubbles and 2-second exposure to 1-MHz 10-μs ultrasound pulsed at 20 Hz and 0.2 – 1 MPa. Enhanced cellular uptake was found for all sizes of molecules tested in this study, although less prominent uptake was observed for larger particles. For all particles, the time window of enhanced cellular uptake could be observed for up to one minute in that study. In an *in vivo* rat brain model, Sheikov *et al.* [77] investigated the duration of blood brain barrier disruption using microbubbles and 30-second exposure to 10-ms 1.5-MHz ultrasound pulsed at 1.1-MPa pressure and 1-Hz pulsing rate. The perfusion of 40-kDa horseradish peroxidase molecules across tight junctions was observed within 4 hours post treatments (Fig. 4c). In an *in vivo* rat eye model, Park *et al.* [78] applied 10-ms 690-kHz ultrasound pulses at 1 Hz pulsing rate and 0.8 – 1.1 MPa pressure for 60 seconds to disrupt the blood retinal barrier. The disruption was evidenced by leakage of a 938-Da magnetic resonance imaging contrast agent (Magnevist) across the barrier. Leakage of Magnevist was visible up to 3.5 hours post ultrasound exposure, suggesting the duration of permeability change on the orders of hours (Fig. 4d).

Importantly, because sonoporation is highly associated with acoustic cavitation of microbubbles, the duration of permeability change may be extended by sustaining the cavitation process with appropriate ultrasound pulsing schemes and/or microbubble parameters. Examples of this idea were demonstrated by Fan *et al.* [66]. They showed that while a single 8-μs 0.17-MPa ultrasound pulse induced sonoporation on a single cell for approximately one minute, an identical second pulse fired approximately two minutes later again excited the microbubbles, inducing another sonoporation event on the same cell. Furthermore, when microbubbles of various sizes were administered, ultrasound pulses of increasing pressures can be delivered sequentially to activate microbubbles of specific sizes at each pulse. This strategy effectively sustained cavitation, and therefore sonoporation, at the target site.

Overall, these studies suggest presence of a temporally variable “window of opportunity” with permeability changes across physiological barriers after a single treatment with ultrasound and microbubbles. This phenomenon suggests a critical point to be considered in treatment planning. To achieve maximum amounts of drug delivery after a single treatment, therapeutic agents should be continuously administered within this temporal window. Such strategy may produce most effective drug delivery outcomes with most efficient use of acoustic energy in each single treatment session.

FUTURE DIRECTIONS

Ultrasound mediated drug delivery has demonstrated its potential to be a useful noninvasive therapeutic tool for various diseases. The advanced knowledge by recent studies, particularly on the spatial distance and temporal window, indicate potential strategies to improve the delivery efficiency for therapeutic use. A few future aspects that may aid the clinical translations of this technique are discussed here.

Spatial Drug Delivery Profile

An ideal drug delivery system would deliver a sufficient dose of drug in the entire target volume. The drug delivery profile of ultrasound mediated drug delivery in the tissues,

however, is not well understood. Stieger *et al.* studied the extravasation of 150-kDa dextran into the interstitium of chicken embryos, and reported a conical or spherical shaped diffusion profile from the extravasation sites [79]. The chicken embryo model, however, only represents a simple environment where the interstitial space was mostly fluid. In a more complex model, e.g., a solid tumor, the interstitial space is composed of densely arranged cells and well-organized collagen and elastic fiber network, which substantially prevent the penetration of drugs. Whether or not a sufficient concentration of drugs can be delivered into the entire target volume as well as the influence of repeated drug delivery to reach the entire target volume needs to be investigated in more complex and clinically relevant animal models.

Development of New Multifunctional Microbubbles

While microbubbles used for ultrasound contrast imaging demonstrate the feasibility of sonoporation, they can be further modified to provide multiple useful features for drug delivery.

The microbubbles can be designed to have optimal cavitation response with minimal requirement of acoustic energy. It is well known that the acoustic properties of microbubbles are highly dependent on several parameters, including diameter, interior gas solubility, shell viscoelasticity, etc. [80]. These parameters may be fine-tuned by changing the shell/core composition or the manufacturing protocol, allowing for optimal acoustic response to ultrasound. For example, Kaya *et al.* developed monodisperse lipid-shelled microbubbles with small size variance using microfluidic flow focusing technique [81]. They found that the acoustic response of the monodisperse microbubbles was significantly enhanced by an optimal combination of the microbubble radius and the ultrasound frequency. This work suggests that development of monodisperse drug loaded microbubbles targeted to specific tissues would allow for cavitation to be generated with minimal ultrasound energy at the specific frequency. Since minimal energy is deposited, the potential adverse effects caused by excessive ultrasound energy may be substantially avoided.

Additionally, microbubbles with improved drug loading capacity need to be developed to increase local drug concentration, propelling diffusive drug transport. A critical factor for the effectiveness of this therapy option is the amount of drugs that can be delivered to the target site, which is directly related to the drug loading capacity of the microbubbles. Currently, there are several drug loading approaches (Fig. 3a). The drugs can be coated on the microbubble surface via electrostatic force [82–86], inserted into the shell during the shell formation process [87–89], loaded in the internal void [90] or in a thick oil layer between the shell and gas core [91, 92]. However, these approaches generally have low drug loading capacity. To enhance the loading capacity, more advanced drug loading approaches are developed. One approach is to coat the microbubbles with multiple layers using a layer-by-layer polyelectrolyte assembly technique, allowing for multifold of drugs to be inserted into the layers [93, 94]. Alternatively, drugs can be loaded on more efficient carrying systems, e.g., liposomes, which are then attached to the microbubbles via a biotin-avidin bridge or a covalent binding [95–97]. While these approaches significantly improve the drug loading capacity, they also modify the shell thickness and composition. The influences of

this modification on the microbubbles' acoustic properties, persistence in the blood circulation, and drug deposition capability *in vivo* need to be further investigated.

Image Guidance for Ultrasound and Microbubble Mediated Drug Delivery

Image guidance and feedback of drug delivery is critical for precisely targeted drug delivery using ultrasound and microbubbles as it allows for adjustment and optimization of the treatment in real time. Since the microbubbles are currently used as contrast agents in ultrasound imaging, the contrast enhanced regions on ultrasound images are useful indicator of the locations of the microbubbles and the loaded drugs. The disappearance of the contrast upon sonication indicates the site of cavitation and drug release. However, the contrast disappears upon destruction of microbubbles, preventing the tracing of the drugs post sonication. To monitor the drug delivery, other imaging modalities, including optical bioluminescence imaging [33, 86] nuclear imaging [98], and magnetic resonance (MR) imaging [99], were adopted. Bioluminescence imaging is less applicable in clinical settings due to its limited penetration depth. Nuclear imaging is less favorable because of the requirement of radioactive materials. So far, MR contrast imaging is the most widely used modality for image guidance of ultrasound and microbubble mediated drug delivery. In this approach, the MR contrast material (e.g., gadolinium) is coinjected into the circulation. Upon disruption of the natural barriers, the contrast material can leak into the targeted tissues, resulting in contrast enhancement on MR images. Although this change on the images indicates disruption of natural barriers for drug delivery, it is only an indirect measurement of drug distribution as the contrast material is not bound to the drug molecules. An imaging approach that can provide anatomical guidance before the treatment, monitor the cavitation process during the treatment, and directly measures the drug distribution post treatment is critical, however, not available so far. Development of such a new imaging approach will be of great value for precise and effective therapy using ultrasound and microbubble mediated drug delivery.

Safety Concerns

Safety concerns in ultrasound and microbubble mediated drug delivery need to be considered before clinical translations. This system involves the use of exogenous agents, microbubbles. Although the microbubbles used for ultrasound contrast imaging have been shown to be very safe and are approved for clinical use, novel drug carrying microbubbles needed to be tested for safety and toxicity. A few studies have shown that cavitation can result in temporary or permanent tissue damage, such as platelet adhesion and thrombus formation [100], and/or reduction of blood flow [101]. These effects need to be carefully studied in different animal models.

CONCLUSIONS

Recent research in ultrasound and microbubble mediated therapeutic delivery provided crucial information regarding the underlying mechanisms behind the physical phenomenon and biological response. The advanced knowledge creates great opportunities to enhance drug delivery into selected tissues/organs. Guided by medical imaging, this technique can be

a very useful tool for precise targeted drug delivery. Such a controlled targeted drug delivery platform may be helpful in many clinically relevant applications.

Acknowledgments

The authors acknowledge support by the Stanford Dean's fellowship award (TYW), the R25 CA118681 grant (KEW), the R01 CA155289-01A1 grant (JKW), and the R01 DK092509-01A1 grant (JKW).

References

1. Szabo, TL. Diagnostic ultrasound imaging: inside out. 2004. Access Online via Elsevier
2. Dubinsky TJ, Cuevas C, Dighe MK, Kolokythas O, Joo HH. High-intensity focused ultrasound: Current potential and oncologic applications. Am J Roentgenology. 2008; 190(1):191–199.
3. Kennedy JE. High-intensity focused ultrasound in the treatment of solid tumours. Nat Rev Cancer. 2005; 5(4):321–327. [PubMed: 15776004]
4. Rassweiler JJ, Knoll T, Kohrmann KU, McAteer JA, Lingeman JE, Cleveland RO, Bailey MR, Chaussy C. Shock wave technology and application: an update. Eur Urol. 2011; 59(5):784–796. [PubMed: 21354696]
5. Roberts WW, Hall TL, Ives K, Wolf JS Jr, Fowlkes JB, Cain CA. Pulsed cavitational ultrasound: a noninvasive technology for controlled tissue ablation (histotripsy) in the rabbit kidney. J Urol. 2006; 175(2):734–738. [PubMed: 16407041]
6. Erdogan O, Esen E. Biological aspects and clinical importance of ultrasound therapy in bone healing. J Ultrasound Med. 2009; 28(6):765–776. [PubMed: 19470817]
7. Tyler WJ. Noninvasive neuromodulation with ultrasound? A continuum mechanics hypothesis. Neuroscientist. 2010; 17(1):25–36. [PubMed: 20103504]
8. Miller DL. Overview of experimental studies of biological effects of medical ultrasound caused by gas body activation and inertial cavitation. Prog Biophys Mol Biol. 2007; 93(1–3):314–330. [PubMed: 16989895]
9. Nyborg WL. Biological effects of ultrasound: development of safety guidelines. Part II: general review. Ultrasound Med Biol. 2001; 27(3):301–333. [PubMed: 11369117]
10. Baker KG, Robertson VJ, Duck FA. A review of therapeutic ultrasound: biophysical effects. Phys Ther. 2001; 81(7):1351–1358. [PubMed: 11444998]
11. Kong G, Dewhirst MW. Hyperthermia and liposomes. Int J Hyperthermia. 1999; 15(5):345–370. [PubMed: 10519688]
12. Song CW. Effect of local hyperthermia on blood flow and microenvironment: a review. Cancer Res. 1984; 44(10 Suppl):4721s–4730s. [PubMed: 6467226]
13. Hahn GM, Strande DP. Cytotoxic effects of hyperthermia and adriamycin on Chinese hamster cells. J Natl Cancer Inst. 1976; 57(5):1063–1067. [PubMed: 1003542]
14. Kong G, Braun RD, Dewhirst MW. Characterization of the effect of hyperthermia on nanoparticle extravasation from tumor vasculature. Cancer Res. 2001; 61(7):3027–3032. [PubMed: 11306483]
15. Lefor AT, Makohon S, Ackerman NB. The effects of hyperthermia on vascular permeability in experimental liver metastasis. J Surg Oncol. 1985; 28(4):297–300. [PubMed: 3982038]
16. Song CW, Park HJ, Lee CK, Griffin R. Implications of increased tumor blood flow and oxygenation caused by mild temperature hyperthermia in tumor treatment. Int J Hyperthermia. 2005; 21(8):761–767. [PubMed: 16338859]
17. Cho CW, Liu Y, Cobb WN, Henthorn TK, Lillehei K, Christians U, Ng KY. Ultrasound-induced mild hyperthermia as a novel approach to increase drug uptake in brain microvessel endothelial cells. Pharm Res. 2002; 19(8):1123–1129. [PubMed: 12240937]
18. Watson KD, Lai CY, Qin S, Kruse DE, Lin YC, Seo JW, Cardiff RD, Mahakian LM, Beegle J, Ingham ES, Curry FR, Reed RK, Ferrara KW. Ultrasound increases nanoparticle delivery by reducing intratumoral pressure and increasing transport in epithelial and epithelial-mesenchymal transition tumors. Cancer Res. 2012; 72(6):1485–1493. [PubMed: 22282664]

19. Koning GA, Eggermont AM, Lindner LH, ten Hagen TL. Hyperthermia and thermosensitive liposomes for improved delivery of chemotherapeutic drugs to solid tumors. Pharm Res. 2010; 27(8):1750–1754. [PubMed: 20424894]
20. Yudina A, Moonen C. Ultrasound-induced cell permeabilisation and hyperthermia: strategies for local delivery of compounds with intracellular mode of action. Int J Hyperthermia. 2012; 28(4): 311–319. [PubMed: 22621733]
21. Gasselhuber A, Dreher MR, Partanen A, Yarmolenko PS, Woods D, Wood BJ, Haemmerich D. Targeted drug delivery by high intensity focused ultrasound mediated hyperthermia combined with temperature-sensitive liposomes: computational modelling and preliminary *in vivo* validation. Int J Hyperthermia. 2012; 28(4):337–348. [PubMed: 22621735]
22. Negussie AH, Yarmolenko PS, Partanen A, Ranjan A, Jacobs G, Woods D, Bryant H, Thomasson D, Dewhirst MW, Wood BJ, Dreher MR. Formulation and characterisation of magnetic resonance imageable thermally sensitive liposomes for use with magnetic resonance-guided high intensity focused ultrasound. Int J Hyperthermia. 2011; 27(2):140–155. [PubMed: 21314334]
23. de Smet M, Heijman E, Langereis S, Hijnen NM, Grull H. Magnetic resonance imaging of high intensity focused ultrasound mediated drug delivery from temperature-sensitive liposomes: an *in vivo* proof-of-concept study. J Control Release. 2011; 150(1):102–110. [PubMed: 21059375]
24. Frenkel V, Etherington A, Greene M, Quijano J, Xie J, Hunter F, Dromi S, Li KC. Delivery of liposomal doxorubicin (Doxil) in a breast cancer tumor model: investigation of potential enhancement by pulsed-high intensity focused ultrasound exposure. Acad Radiol. 2006; 13(4): 469–479. [PubMed: 16554227]
25. O'Neill BE, Vo H, Angstadt M, Li KP, Quinn T, Frenkel V. Pulsed high intensity focused ultrasound mediated nanoparticle delivery: mechanisms and efficacy in murine muscle. Ultrasound Med Biol. 2009; 35(3):416–424. [PubMed: 19081668]
26. Fujii H, Matkar P, Liao C, Rudenko D, Lee PJ, Kuliszewski MA, Prud'homme GJ, Leong-Poi H. Optimization of Ultrasound-mediated Anti-angiogenic Cancer Gene Therapy. Mol Ther Nucleic Acids. 2013; 2(e94):1–9.
27. Tsai K-C, Liao Z-K, Lin W-L, Shieh M-J, Hwang L-H, Chen W-S. Antiangiogenic Gene Therapy on Hepatocellular Carcinoma Using Endostatin and Sonoporation *in vivo*. Biomed Eng Appl Basis Commun. 2010; 22(1):71–79.
28. Chen S, Ding JH, Bekeredjian R, Yang BZ, Shohet RV, Johnston SA, Hohmeier HE, Newgard CB, Grayburn PA. Efficient gene delivery to pancreatic islets with ultrasonic microbubble destruction technology. Proc Natl Acad Sci USA. 2006; 103(22):8469–8474. [PubMed: 16709667]
29. Hynynen K. Ultrasound for drug and gene delivery to the brain. Adv Drug Deliv Rev. 2008; 60(10):1209–1217. [PubMed: 18486271]
30. Treat LH, McDannold N, Zhang Y, Vykhodtseva N, Hynynen K. Improved anti-tumor effect of liposomal doxorubicin after targeted blood-brain barrier disruption by MRI-guided focused ultrasound in rat glioma. Ultrasound Med Biol. 2012; 38(10):1716–1725. [PubMed: 22818878]
31. Ting CY, Fan CH, Liu HL, Huang CY, Hsieh HY, Yen TC, Wei KC, Yeh CK. Concurrent blood-brain barrier opening and local drug delivery using drug-carrying microbubbles and focused ultrasound for brain glioma treatment. Biomaterials. 2012; 33(2):704–712. [PubMed: 22019122]
32. Newman CM, Bettinger T. Gene therapy progress and prospects: ultrasound for gene transfer. Gene Ther. 2007; 14(6):465–475. [PubMed: 17339881]
33. Panje CM, Wang DS, Willmann JK. Ultrasound and Microbubble-Mediated Gene Delivery in Cancer: Progress and Perspectives. Invest Radiol. 2013; 48(11):755–769. [PubMed: 23697924]
34. Kaneko OF, Willmann JK. Ultrasound for molecular imaging and therapy in cancer. Quant Imaging Med Surg. 2012; 2(2):87–97. [PubMed: 23061039]
35. Castle J, Butts M, Healey A, Kent K, Marino M, Feinstein SB. Ultrasound-mediated targeted drug delivery: recent success and remaining challenges. Am J Physiol Heart Circ Physiol. 2013; 304(3):H350–357. [PubMed: 23203969]
36. Yoon CS, Park JH. Ultrasound-mediated gene delivery. Expert Opin Drug Deliv. 2010; 7(3):321–330. [PubMed: 20166854]
37. Deshpande N, Needles A, Willmann JK. Molecular ultrasound imaging: current status and future directions. Clin Radiol. 2010; 65(7):567–581. [PubMed: 20541656]

38. Kircher MF, Willmann JK. Molecular body imaging: MR imaging, CT, and US. part I. principles. Radiology. 2012; 263(3):633–643. [PubMed: 22623690]
39. Kiessling F, Huppert J, Palmowski M. Functional and molecular ultrasound imaging: concepts and contrast agents. Curr Med Chem. 2009; 16(5):627–642. [PubMed: 19199927]
40. Klibanov AL. Preparation of targeted microbubbles: ultrasound contrast agents for molecular imaging. Med Biol Eng Comput. 2009; 47(8):875–882. [PubMed: 19517153]
41. Pysz MA, Willmann JK. Targeted contrast-enhanced ultrasound: an emerging technology in abdominal and pelvic imaging. Gastroenterology. 2011; 140(3):785–790. [PubMed: 21255573]
42. Leighton, TG. The acoustic bubble. Academic Press; 1997.
43. Collis J, Manasseh R, Liovic P, Tho P, Ooi A, Petkovic-Duran K, Zhu Y. Cavitation microstreaming and stress fields created by microbubbles. Ultrasonics. 2010; 50(2):273–279. [PubMed: 19896683]
44. Nyborg WL. Ultrasonic microstreaming and related phenomena. Br J Cancer Suppl. 1982; 5:156–160. [PubMed: 6950752]
45. Lauterborn W, Bolle H. Experimental investigations of cavitation-bubble collapse in the neighbourhood of a solid boundary. J Fluid Mech. 1975; 72(02):391–393.
46. Coleman AJ, Saunders JE, Crum LA, Dyson M. Acoustic cavitation generated by an extracorporeal shockwave lithotripter. Ultrasound Med Biol. 1987; 13(2):69–76. [PubMed: 3590362]
47. Postema M, van Wamel A, ten Cate FJ, de Jong N. High-speed photography during ultrasound illustrates potential therapeutic applications of microbubbles. Med Phys. 2005; 32(12):3707–3711. [PubMed: 16475770]
48. Church CC. A theoretical study of cavitation generated by an extracorporeal shock wave lithotripter. J Acoust Soc Am. 1989; 86(1):215–227. [PubMed: 2754108]
49. Lauterborn W, Ohl CD. Cavitation bubble dynamics. Ultrason Sonochem. 1997; 4(2):65–75. [PubMed: 11237047]
50. Morgan KE, Allen JS, Dayton PA, Chomas JE, Klibaov AL, Ferrara KW. Experimental and theoretical evaluation of microbubble behavior: effect of transmitted phase and bubble size. IEEE Trans Ultrason Ferroelectr Freq Control. 2000; 47(6):1494–1509. [PubMed: 18238696]
51. Chomas JE, Dayton P, May D, Ferrara K. Threshold of fragmentation for ultrasonic contrast agents. J Biomed Opt. 2001; 6(2):141–150. [PubMed: 11375723]
52. Bouakaz A, Versluis M, de Jong N. High-speed optical observations of contrast agent destruction. Ultrasound Med Biol. 2005; 31(3):391–399. [PubMed: 15749563]
53. Ferrara K, Pollard R, Borden M. Ultrasound microbubble contrast agents: fundamentals and application to gene and drug delivery. Annu Rev Biomed Eng. 2007; 9:415–447. [PubMed: 17651012]
54. Lauterborn W, Kurz T, Geisler R, Schanz D, Lindau O. Acoustic cavitation, bubble dynamics and sonoluminescence. Ultrason Sonochem. 2007; 14(4):484–491. [PubMed: 17254826]
55. de Jong N, Emmer M, van Wamel A, Versluis M. Ultrasonic characterization of ultrasound contrast agents. Med Biol Eng Comput. 2009; 47(8):861–873. [PubMed: 19468770]
56. Skyba DM, Price RJ, Linka AZ, Skalak TC, Kaul S. Direct *in vivo* visualization of intravascular destruction of microbubbles by ultrasound and its local effects on tissue. Circulation. 1998; 98(4): 290–293. [PubMed: 9711932]
57. Prentice P, Cuschieri A, Dholakia K, Prausnitz M, Campbell P. Membrane disruption by optically controlled microbubble cavitation. Nat Phys. 2005; 1(2):107–110.
58. Ohl CD, Arora M, Ikink R, de Jong N, Versluis M, Delius M, Lohse D. Sonoporation from jetting cavitation bubbles. Biophys J. 2006; 91(11):4285–4295. [PubMed: 16950843]
59. Nyborg W, Miller D. Biophysical implications of bubble dynamics. Appl Sci Res. 1982; 38(1):17–24.
60. Marmottant P, Hilgenfeldt S. Controlled vesicle deformation and lysis by single oscillating bubbles. Nature. 2003; 423(6936):153–156. [PubMed: 12736680]
61. Wang C, Jalikop SV, Hilgenfeldt S. Size-sensitive sorting of microparticles through control of flow geometry. Appl Phys Lett. 2011; 99(3):034101.

62. Ferrara KW, Borden MA, Zhang H. Lipid-shelled vehicles: engineering for ultrasound molecular imaging and drug delivery. Acc Chem Res. 2009; 42(7):881–892. [PubMed: 19552457]
63. Sirsi S, Borden M. Microbubble Compositions, Properties and Biomedical Applications. Bubble Sci Eng Technol. 2009; 1(1–2):3–17. [PubMed: 20574549]
64. Hernot S, Klibanov AL. Microbubbles in ultrasound-triggered drug and gene delivery. Adv Drug Deliv Rev. 2008; 60(10):1153–1166. [PubMed: 18486268]
65. Lentacker I, De Smedt SC, Sanders NN. Drug loaded microbubble design for ultrasound triggered delivery. Soft Matter. 2009; 5(11):2161–2170.
66. Fan Z, Liu H, Mayer M, Deng CX. Spatiotemporally controlled single cell sonoporation. Proc Natl Acad Sci USA. 2012; 109(41):16486–16491. [PubMed: 23012425]
67. Kudo N, Okada K, Yamamoto K. Sonoporation by single-shot pulsed ultrasound with microbubbles adjacent to cells. Biophys J. 2009; 96(12):4866–4876. [PubMed: 19527645]
68. Zhou Y, Kumon RE, Cui J, Deng CX. The size of sonoporation pores on the cell membrane. Ultrasound Med Biol. 2009; 35(10):1756–1760. [PubMed: 19647924]
69. Chen H, Kreider W, Brayman AA, Bailey MR, Matula TJ. Blood vessel deformations on microsecond time scales by ultrasonic cavitation. Phys Rev Lett. 2011; 106(3):034301. [PubMed: 21405276]
70. Chen H, Brayman AA, Kreider W, Bailey MR, Matula TJ. Observations of translation and jetting of ultrasound-activated microbubbles in mesenteric microvessels. Ultrasound Med Biol. 2011; 37(12):2139–2148. [PubMed: 22036639]
71. Chen H, Brayman AA, Evan AP, Matula TJ. Preliminary observations on the spatial correlation between short-burst microbubble oscillations and vascular bioeffects. Ultrasound Med Biol. 2012; 38(12):2151–2162. [PubMed: 23069136]
72. Gac SL, Zwaan E, van den Berg A, Ohl CD. Sonoporation of suspension cells with a single cavitation bubble in a microfluidic confinement. Lab Chip. 2007; 7(12):1666–1672. [PubMed: 18030385]
73. Jain RK. Determinants of tumor blood flow: a review. Cancer Res. 1988; 48(10):2641–2658. [PubMed: 3282647]
74. Shortencarier MJ, Dayton PA, Bloch SH, Schumann PA, Matsunaga TO, Ferrara KW. A method for radiation-force localized drug delivery using gas-filled lipospheres. IEEE Trans Ultrason Ferroelectr Freq Control. 2004; 51(7):822–831. [PubMed: 15301001]
75. Xie A, Belcik T, Qi Y, Morgan TK, Champaneri SA, Taylor S, Davidson BP, Zhao Y, Klibanov AL, Kuliszewski MA, Leong-Poi H, Ammi A, Lindner JR. Ultrasound-mediated vascular gene transfection by cavitation of endothelial-targeted cationic microbubbles. JACC Cardiovasc Imaging. 2012; 5(12):1253–1262. [PubMed: 23236976]
76. Van Wamel A, Bouakaz A, de Jong N. Duration of ultrasound bubbles enhanced cell membrane permeability. Proc IEEE Ultrason Symp. 2003; 1:917–920.
77. Sheikov N, McDannold N, Sharma S, Hynynen K. Effect of focused ultrasound applied with an ultrasound contrast agent on the tight junctional integrity of the brain microvascular endothelium. Ultrasound Med Biol. 2008; 34(7):1093–1104. [PubMed: 18378064]
78. Park J, Zhang Y, Vykhodtseva N, Akula JD, McDannold NJ. Targeted and reversible blood-retinal barrier disruption via focused ultrasound and microbubbles. PLoS One. 2012; 7(8):e42754. [PubMed: 22912733]
79. Stieger SM, Caskey CF, Adamson RH, Qin S, Curry FR, Wisner ER, Ferrara KW. Enhancement of vascular permeability with low-frequency contrast-enhanced ultrasound in the chorioallantoic membrane model. Radiology. 2007; 243(1):112–121. [PubMed: 17392250]
80. Hoff, L. Acoustic characterization of contrast agents for medical ultrasound imaging. Kluwer Academic Pub; 2001.
81. Kaya M, Feingold S, Hettiarachchi K, Lee AP, Dayton PA. Acoustic responses of monodisperse lipid-encapsulated microbubble contrast agents produced by flow focusing. Bubble Sci Eng Technol. 2010; 2(2):33–40. [PubMed: 21475641]
82. Kipshidze NN, Porter TR, Dangas G, Yazdi H, Tio F, Xie F, Hellinga D, Wolfram R, Seabron R, Waksman R, Abizaid A, Roubin G, Iyer S, Colombo A, Leon MB, Moses JW, Iversen P. Novel site-specific systemic delivery of Rapamycin with perfluorobutane gas microbubble carrier

reduced neointimal formation in a porcine coronary restenosis model. Catheter Cardiovasc Interv. 2005; 64(3):389–394. [PubMed: 15736246]

83. Shohet RV, Chen S, Zhou YT, Wang Z, Meidell RS, Unger RH, Grayburn PA. Echocardiographic destruction of albumin microbubbles directs gene delivery to the myocardium. Circulation. 2000; 101(22):2554–2556. [PubMed: 10840004]
84. Christiansen JP, French BA, Klibanov AL, Kaul S, Lindner JR. Targeted tissue transfection with ultrasound destruction of plasmid-bearing cationic microbubbles. Ultrasound Med Biol. 2003; 29(12):1759–1767. [PubMed: 14698343]
85. Haag P, Frauscher F, Gradl J, Seitz A, Schafer G, Lindner JR, Klibanov AL, Bartsch G, Klocker H, Eder IE. Microbubble-enhanced ultrasound to deliver an antisense oligodeoxynucleotide targeting the human androgen receptor into prostate tumours. J Steroid Biochem Mol Biol. 2006; 102(1–5): 103–113. [PubMed: 17055720]
86. Wang DS, Panje C, Pysz MA, Paulmurugan R, Rosenberg J, Gambhir SS, Schneider M, Willmann JK. Cationic versus neutral microbubbles for ultrasound-mediated gene delivery in cancer. Radiology. 2012; 264(3):721–732. [PubMed: 22723497]
87. Frenkel PA, Chen S, Thai T, Shohet RV, Grayburn PA. DNA-loaded albumin microbubbles enhance ultrasound-mediated transfection. in vitro Ultrasound Med Biol. 2002; 28(6):817–822.
88. Teupe C, Richter S, Fisslthaler B, Randriamboavonjy V, Ihling C, Fleming I, Busse R, Zeiher AM, Dimmeler S. Vascular gene transfer of phosphomimetic endothelial nitric oxide synthase (S1177D) using ultrasound-enhanced destruction of plasmid-loaded microbubbles improves vasoreactivity. Circulation. 2002; 105(9):1104–1109. [PubMed: 11877363]
89. Bekeredjian R, Chen S, Grayburn PA, Shohet RV. Augmentation of cardiac protein delivery using ultrasound targeted microbubble destruction. Ultrasound Med Biol. 2005; 31(5):687–691. [PubMed: 15866418]
90. Huang SL, MacDonald RC. Acoustically active liposomes for drug encapsulation and ultrasound-triggered release. Biochim Biophys Acta. 2004; 1665(1–2):134–141. [PubMed: 15471579]
91. Unger EC, McCreery TP, Sweitzer RH, Caldwell VE, Wu Y. Acoustically active lipospheres containing paclitaxel: a new therapeutic ultrasound contrast agent. Invest Radiol. 1998; 33(12): 886–892. [PubMed: 9851823]
92. Tartis MS, McCallan J, Lum AF, LaBell R, Stieger SM, Matsunaga TO, Ferrara KW. Therapeutic effects of paclitaxel-containing ultrasound contrast agents. Ultrasound Med Biol. 2006; 32(11): 1771–1780. [PubMed: 17112963]
93. Shchukin DG, Kohler K, Mohwald H, Sukhorukov GB. Gas-filled polyelectrolyte capsules. Angew Chem Int Ed Engl. 2005; 44(21):3310–3314. [PubMed: 15844113]
94. Borden MA, Caskey CF, Little E, Gillies RJ, Ferrara KW. DNA and polylysine adsorption and multilayer construction onto cationic lipid-coated microbubbles. Langmuir. 2007; 23(18):9401–9408. [PubMed: 17665937]
95. Kheirolomoom A, Dayton PA, Lum AF, Little E, Paoli EE, Zheng H, Ferrara KW. Acoustically-active microbubbles conjugated to liposomes: characterization of a proposed drug delivery vehicle. J Control Release. 2007; 118(3):275–284. [PubMed: 17300849]
96. Vandenbroucke RE, Lentacker I, Demeester J, De Smedt SC, Sanders NN. Ultrasound assisted siRNA delivery using PEG-siPlex loaded microbubbles. J Control Release. 2008; 126(3):265–273. [PubMed: 18237813]
97. Kim DH, Klibanov AL, Needham D. The influence of tiered layers of surface-grafted poly (ethylene glycol) on receptor-ligand-mediated adhesion between phospholipid monolayer-stabilized microbubbles and coated glass beads. Langmuir. 2000; 16(6):2808–2817.
98. Khaibullina A, Jang BS, Sun H, Le N, Yu S, Frenkel V, Carrasquillo JA, Pastan I, Li KC, Paik CH. Pulsed high-intensity focused ultrasound enhances uptake of radiolabeled monoclonal antibody to human epidermoid tumor in nude mice. J Nucl Med. 2008; 49(2):295–302. [PubMed: 18199622]
99. Hynynen K, McDannold N, Vykhodtseva N, Jolesz FA. Noninvasive MR imaging-guided focal opening of the blood-brain barrier in rabbits. Radiology. 2001; 220(3):640–646. [PubMed: 11526261]
100. Kuijpers MJ, Gilio K, Reitsma S, Nergiz-Unal R, Prinzen L, Heeneman S, Lutgens E, van Zandvoort MA, Nieswandt B, Egbrink MG, Heemskerk JW. Complementary roles of platelets

and coagulation in thrombus formation on plaques acutely ruptured by targeted ultrasound treatment: a novel intravital model. J Thromb Haemost. 2009; 7(1):152–161. [PubMed: 18983512]

101. Hu X, Kheirolomoom A, Mahakian LM, Beegle JR, Kruse DE, Lam KS, Ferrara KW. Insonation of targeted microbubbles produces regions of reduced blood flow within tumor vasculature. Invest Radiol. 2012; 47(7):398–405. [PubMed: 22659591]

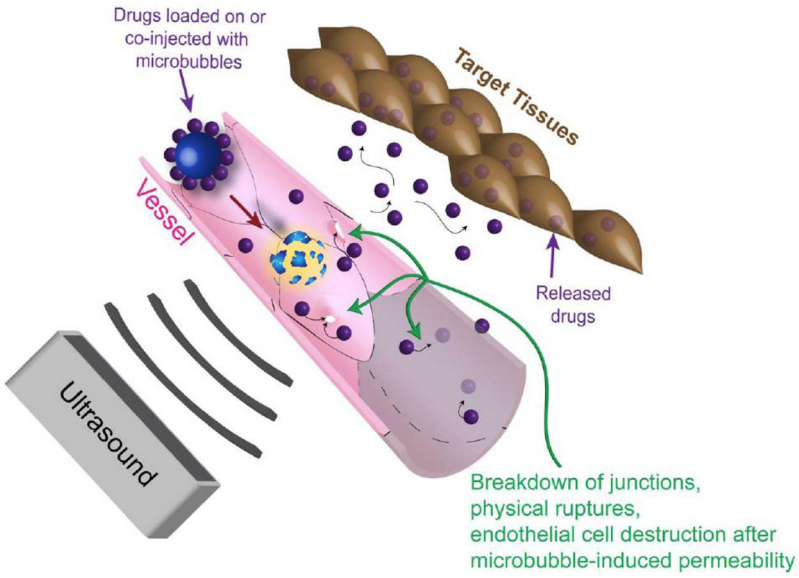

Fig. 1.

Schematic drawing of ultrasound guided drug delivery. Ultrasound triggers microbubble cavitation at its focus, causing breakdown of tight junctions, opening on cellular membrane, and/or vessel disruption. These phenomena induce permeability change on the cells and vessels, allowing for drug delivery in a spatially localized region.

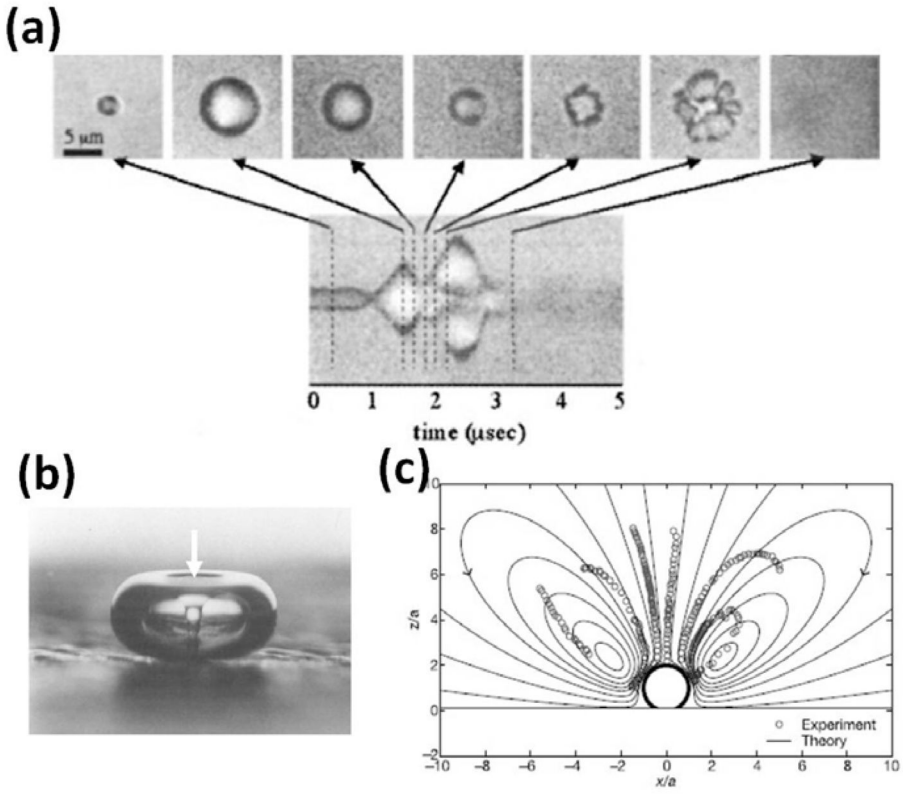

Fig. 2.

Ultrasound induced microbubble cavitation and fluid motions. (**a**) Microbubbles undergo volumetric expansion, contraction, fragmentation, and coalesce in response to the insonation ultrasound. They may continue to expand for several to several hundreds of microseconds and then collapse or dissolve after ultrasound is ceased. (**b**) During the violent collapse of microbubbles, fluid jets can form and impinge into a nearby surface. In this example, a fluid jet (white arrow) was formed in the center of a 2-mm bubble during the collapse and impinged into the surface where the bubble rested on. (**c**) The microbubble cavitation may induce local fluid motion called microstreaming. This example shows a computed fluid flow (solid lines) superimposed with measured flow (dots) near a microbubble undergoing volumetric oscillation. Figure panels (**a**), (**b**), and (**c**) are reprinted with permission from references [51, 46, 60], respectively.

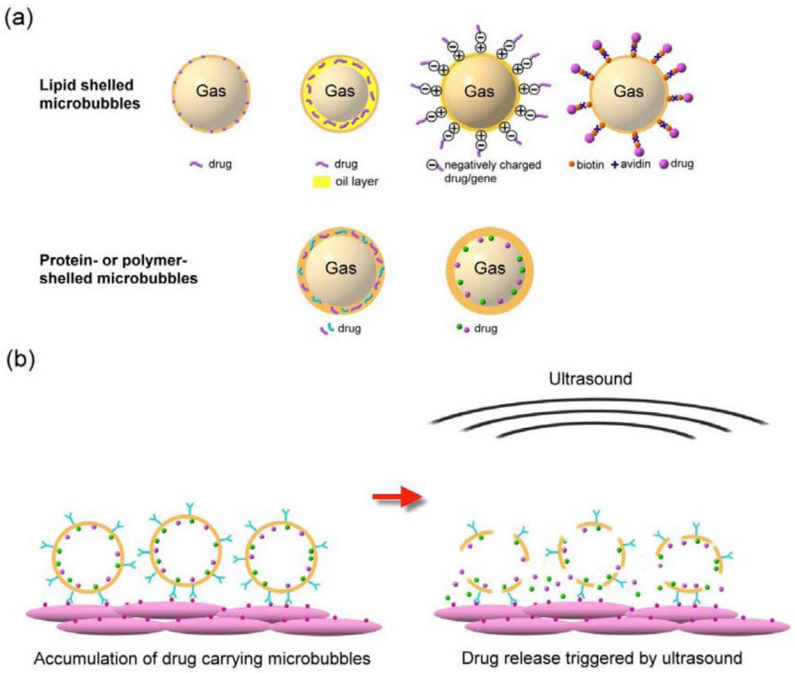

Fig. 3.

(**a**) Examples of drug loading strategies. The drugs can be loaded on the shell of microbubbles, embedded in the shell matrix, or loaded in the internal void. For lipid-shelled microbubbles, the drug can be inserted in the lipid shell, in a thick oil layer underneath the lipid shell, on a positively charged shell through electrostatic force (for example, binding plasmid to cationic microbubble [86]), bonded to the shell via a biotin-avidin bridging system (for example, attaching liposomes to microbubbles using the bridging system [95]) or through covalent binding approaches (for example, adhering particles to microbubbles using a polymer [97]). For protein- or polymer-shelled microbubbles, the drug can be entrapped in the thick cross-linked protein or polymer matrix, or loaded in the internal void. (**b**) Surface modification of microbubbles allows for specific binding to cells at target sites, increasing local drug concentration. Application of ultrasound locally triggers the release of the accumulated drugs in the focal region.

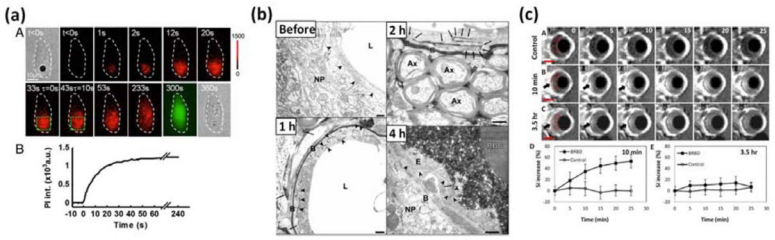

Fig. 4.

Temporally resolved sonoporation process in (**a**) a cultured cell [66], (**b**) blood brain barrier disruption [77], and (**c**) blood-retinal barrier disruption [78]. (**a**) Increased red color indicates increased uptake of propidium iodide into the cell. Such uptake occurred most significantly within the first minute after ultrasound exposure, and gradually saturate at four minutes, indicating a resealing process. (**b**) Leakage of horseradish peroxidase molecules (black color) across the tight junctions was observed 1 h and 2 h after ultrasound and microbubble treatment, and was restored 4 h post treatment. (**c**) Enhanced contrast on MR images indicates perfusion of Magnevist across the barrier 10 minutes and 3.5 h after ultrasound and microbubble treatment. Overall, while a single bubble cavitation event induced by a short (8 μs) low intensity (0.17MPa) ultrasound can induce cellular uptake of propidium iodide for several minutes, exposure to long (10 ms) higher intensity (0.8–1 MPa) ultrasound pulses for a longer time (30 seconds) can induce permeability change across the natural barriers for up to 4 hours. Figure panels (**a**), (**b**), and (**c**) are reprinted with permission from references [66, 67], and [78], respectively.